Assistive torque design for hip-joint exoskeleton by admittance shaping using loop shaping method

***Abstract*—Hip joints provide more energy for walking forward, while at knee joints, elastic structures perform much of the cyclic work, saving and putting out energy. Therefore, for assistive exoskeletons, designing appropriate torque curve to actuate its hip joints is especially important. Nevertheless, the design of the hip assistive torque profile should take the knee joints into consideration. This paper presents a method to generate assistive torque for hip joints of lower limb exoskeletons, which is based on the dynamics of the whole leg. The worn exoskeleton is treated as an outer source to the wearer, and it would modify the wear's torque-to-angle relationship, namely admittance. By employing a loop-shaping method, the admittance of the leg is changed to the desired profile and the assistive torque for the hip joint is determined accordingly.**

***Index Terms*—Exoskeleton, Admittance control, Loop shaping.**

I. Introduction

As the development of exoskeletons goes on, associated controllers of various kinds have been developed at the same time. There are two typical traditional methods that have been widely applied, predefined trajectory tracking method and zero torque method, namely transparent mode. Predefined trajectory tracking method is suitable for early-stage lower limb rehabilitation, where exoskeletons lead patients suffering paraplegia or lower-limb impairment in robot-in-charge mode. Zero torque control is usually selected in systems designed for load-carrying, which is actually a passive work mode.

The two widely used methods have several drawbacks. In most cases where predefined trajectory tracking method is applied, the exoskeleton system with such a controller is designed to work with a treadmill in a platform-based working manner. Since the set trajectory is predefined, the wearer can only walk with the exoskeleton system in a uniform speed determined in the controller. More importantly, the controller may not be helpful for systems designed for able-bodied individuals. During human walking at preferred walking speeds, the swing leg behaves as a physical pendulum driven close to its natural frequency. Utilizing the natural pendular dynamics of the swing leg minimizes muscle work and allows movement control through a more economic alternative: muscle force. As for the stance limb, it guides the center of mass along a trajectory similar to an inverted pendulum, allowing cyclic exchange of gravitational potential energy and kinetic energy. An inverted pendulum is energy conservative and theoretically requires zero mechanical work during single support. Humans use this strategy for walking to save energy. As a result, elastic structures perform much of the cyclic work at a joint. Therefore, for an able-bodied individual with his own motion intention, a leading exoskeleton system in trajectory tracking manner may not be assistive or comfortable, since the leg muscle does not perform positive work during the whole gait cycle. Only patients suffering lower limb disability or weakness can benefits from the controller.

Zero torque control relies on interactive torque measurement. The method reduces the burden on the wearers by compensating the gravity, friction of the system and the interaction force between the system and the wearer. Although used for able-bodied subjects, it cannot perform net positive work to the leg. When walking with the exoskeleton system, the wearer still provides all the energy and even more energy needed for walking forward than walking without the system. Besides, the gravity and friction compensation comes from model prediction, while the interaction force compensation is based on the force/torque sensor results. However, the measurement error is inevitable, and it is often difficult to calibrate the sensors because of the complex coupling and the varying initial value when standing still in the exoskeleton system.

Because of these drawbacks, there comes the need for more intelligent exoskeleton controllers. Adaptive oscillators-based control predicts the suitable force of next movement of legs using gait information. Fuzzy controller is an attempt to build neurologically inspired bio-mechanical models, which can return the desired movements by merging different bio-mechanical signals. Proportional myoelectrical control is another widely used method, where the desired output of the actuators is proportional to the processed EMG signal of a selected muscle.

Among these controllers, Aguirre's group proposes a model based method. They define assistance as a desired dynamic response for the human leg. The work is based on the principle that wearing the exoskeleton can be seen as replacing the leg's natural admittance with the equivalent admittance of the coupled system. The control goal is to make the leg obey a desired admittance model.

This admittance shaping control is promising. It can let wearers feel flexible and free while being assisted and provides assistance independently of the specific motion attempted. Namely, except for assisting normal walking, the controller allows to assist other lower-limb movements like gait initiation and reactive stepping.

However, there lie several limitations in their work. The model is built by treating the whole human limb as a 1-DOF linear pendulum which is simplified too much. And on the basis of this 1-DOF linear pendulum, the impedance of the leg at the hip joint, namely the transfer function relating the net muscle torque acting on that joint to the resulting angular velocity of the leg, is simply formulated with three constant coefficients, the hip joint stiffness coefficient k, the hip joint damping coefficient b and the moment of inertia of

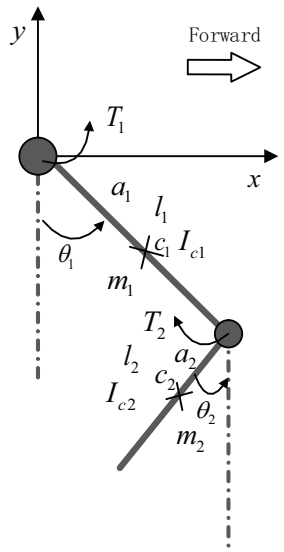

Fig. 1. A diagram of the swing leg

the extended leg about the hip I. Since these three coefficients are definitely varying during a gait cycle, the model with constant coefficients is not convictive enough. In addition, the muscle torque of the thigh is supposed to be related to the kinetic status of the shank, so an impedance model of the hip joint without considering the knee joint is disputable.

In this paper, we build a model considering the knee joint to design assistive torque profile for the hip joint. The admittance formulation is obtained with Lagrange function by analyzing the kinetics of the swing leg with two joints rotating around their center respectively. The assistance from the exoskeleton system is regarded as a modification to the admittance, namely the torque-to-angle relationship. The admittance is modified by using loop shaping method.

II. Dynamic Model

The kinetic energy of the thigh is

$$T_1 = \frac{1}{2} J_{o1} \dot{\theta_1}^2 \tag{1}$$

where

$$J_{o1} = J_{c1} + m_1 a_1^2 \tag{2}$$

The kinetic energy of the shank is

$$T_2 = \frac{1}{2} m_2 v_{c2}^2 + \frac{1}{2} J_{c2} \dot{\theta_2}^2 \tag{3}$$

where v_{c2} can be obtained by the following equations,

$$\begin{cases} x_{c2} = l_1 \sin\theta_1 + a_2 \sin\theta_2 \\ y_{c2} = -l_1 \cos\theta_1 - a_2 \cos\theta_2 \end{cases} \tag{4}$$

$$\begin{cases} \dot{x_{c2}} = l_1 \dot{\theta_1} \cos\theta_1 + a_2 \dot{\theta_2} \cos\theta_2 \\ \dot{y_{c2}} = l_1 \dot{\theta_1} \sin\theta_1 + a_2 \dot{\theta_2} \sin\theta_2 \end{cases} \tag{5}$$

Then

$$v_{c2}^2 = \dot{x_{c2}}^2 + \dot{y_{c2}}^2 = l_1^2 \dot{\theta_1}^2 + a_2^2 \dot{\theta_2}^2 + 2 l_1 a_2 \dot{\theta_1} \dot{\theta_2} \cos(\theta_1 - \theta_2) \tag{6}$$

Then the kinetic energy of the shank can be obtained as

$$T_2 = \frac{1}{2} m_2 l_1^2 \dot{\theta_1}^2 + \frac{1}{2} (J_{c2} + m_2 a_2^2) \dot{\theta_2}^2 + m_2 l_1 a_2 \dot{\theta_1} \dot{\theta_2} \cos(\theta_1 - \theta_2) \tag{7}$$

According to the Force Transfer Theorem, the gravitational potential energy of the lower limb is

$$V = -m_1 g a_1 \cos\theta_1 - m_2 g (l_1 \cos\theta_1 + a_2 \cos\theta_2) \tag{8}$$

Then the Lagrange function of the lower limb can be obtained as

$$\begin{aligned} L &= T - V \\ &= T_1 + T_2 - V \\ &= \frac{1}{2}(J_{o1} + m_2 l_1^2) \dot{\theta_1}^2 \\ &+ \frac{1}{2}(J_{c2} + m_2 a_2^2) \dot{\theta_2}^2 \\ &+ m_2 l_1 a_2 \dot{\theta_1} \dot{\theta_2} \cos(\theta_1 - \theta_2) \\ &+ (m_1 a_1 + m_2 l_1 g \cos\theta_1 + m_2 a_2 g \cos\theta_2 \end{aligned} \tag{9}$$

The torques are

$$\begin{cases} \frac{d}{dt}(\frac{\partial L}{\partial \dot{\theta_1}}) - \frac{\partial L}{\partial \theta_1} = T_1 \\ \frac{d}{dt}(\frac{\partial L}{\partial \dot{\theta_2}}) - \frac{\partial L}{\partial \theta_2} = T_2 \end{cases} \tag{10}$$

Linearize the Lagrange Function (mainly the trigonometric function parts) to obtain the torque formulation.

$$\begin{aligned} L &= \frac{1}{2}(J_{o1} + m_2 l_1^2) \dot{\theta_1}^2 \\ &+ \frac{1}{2}(J_{c2} + m_2 a_2^2) \dot{\theta_2}^2 \\ &+ m_2 l_1 a_2 \dot{\theta_1} \dot{\theta_2} \{1 - \frac{1}{2}(\theta_2 - \theta_1)^2 + O[(\theta_2 - \theta_1)^4]\} \\ &+ (m_1 a_1 + m_2 l_1 g \{1 - \frac{1}{2}(\theta_1)^2 + O(\theta_1^4)\} \\ &+ m_2 a_2 g \{1 - \frac{1}{2}(\theta_2)^2 + O(\theta_2^4)\} \\ &= \frac{1}{2}[\dot{\theta_1}\ \dot{\theta_2}] M \begin{bmatrix} \dot{\theta_1} \\ \dot{\theta_2} \end{bmatrix} - \frac{1}{2}[\theta_1\ \theta_2] K \begin{bmatrix} \theta_1 \\ \theta_2 \end{bmatrix} \end{aligned} \tag{11}$$

where M is the positive definite symmetric mass matrix

$$M = \begin{bmatrix} J_{o1} + m_2 l_1^2 & m_2 l_1 a_2 \\ m_2 l_1 a_2 & J_{c2} + m_2 a_2^2 \end{bmatrix} \tag{12}$$

where K is the positive definite symmetric stiffness matrix

$$K = g \begin{bmatrix} m_1 a_1 + m_2 l_1 & 0 \\ 0 & m_2 a_2 \end{bmatrix} \tag{13}$$

Then the torque matrix is obtained by substituting (11) into (10).

$$M \begin{bmatrix} \ddot{\theta_1} \\ \ddot{\theta_2} \end{bmatrix} + K \begin{bmatrix} \theta_1 \\ \theta_2 \end{bmatrix} = \begin{bmatrix} T_1 \\ T_2 \end{bmatrix} \tag{14}$$

The system model is given as

$$\begin{bmatrix} \ddot{\theta_1} \\ \ddot{\theta_2} \end{bmatrix} + M^{-1} K \begin{bmatrix} \theta_1 \\ \theta_2 \end{bmatrix} = M^{-1} \begin{bmatrix} T_1 \\ T_2 \end{bmatrix} \tag{15}$$

Add the damping term.

$$\begin{bmatrix} \ddot{\theta_1} \\ \ddot{\theta_2} \end{bmatrix} + \begin{bmatrix} b_1 \dot{\theta_1} \\ b_2 \dot{\theta_2} \end{bmatrix} + \hat{K} \begin{bmatrix} \theta_1 \\ \theta_2 \end{bmatrix} = \hat{M} \begin{bmatrix} T_1 \\ T_2 \end{bmatrix} \tag{16}$$

where $\hat{K} = M^{-1}K, \hat{M} = M^{-1}$

Ignoring the actuating torque of the knee joint, let $T_2 = 0$. After the Laplace Transformation,

$$\begin{cases} s^2\Theta_1(s) + b_1 s\Theta_1(s) + \hat{K}_{11}\Theta_1(s) + \hat{K}_{12}\Theta_2(s) = \hat{M}_{11}T_1(s) \\ s^2\Theta_2(s) + b_2 s\Theta_2(s) + \hat{K}_{21}\Theta_1(s) + \hat{K}_{22}\Theta_2(s) = \hat{M}_{21}T_1(s) \end{cases}$$

Solve $\Theta_1(s), \Theta_2(s)$ from the equations, and the formulation of $\Theta_1(s)$ can be obtained by substituting $\Theta_2(s)$ into $\Theta_1(s)$. Then the Transfer Function from $T_1(s)$ to $\Theta_1(s)$ can be obtained.

$$\Theta_1(s) = \frac{\hat{M}_{11}(s^2 + b_2 s + \hat{K}_{22}) - \hat{K}_{12}\hat{M}_{21}}{(s^2 + b_1 s + \hat{K}_{11})(s^2 + b_2 s + \hat{K}_{22}) - \hat{K}_{12}\hat{K}_{21}} T_1(s) \tag{18}$$

III. Lower-limb Assistance by Loop Shaping: Control Design

A. Target Frequency Response Specifying

According to the Lagrange equation above, we have already derived the human limb's integral mechanical admittance, $X_h(s) = Y_h(s)/s$, with matrices defined in early sections, we can express the integral mechanical admittance as follows:

$$X_h = \frac{\hat{M}_{11}(s^2 + b_2 s + \hat{K}_{22}) - \hat{K}_{12}\hat{M}_{21}}{(s^2 + b_1 s + \hat{K}_{11})(s^2 + b_2 s + \hat{K}_{22}) - \hat{K}_{12}\hat{K}_{21}} \tag{19}$$

According to the frequency response of the integral mechanical admittance, we can find two peaks in Fig.2. We then define three dimensionless control parameters R_w(frequency ratio),R_M(resonant ratio) and R_{DC}(DC gain ratio) which run through the whole article.

$$R_w = \frac{w_d}{w_h} \tag{20}$$

$$R_M = \frac{M_d}{M_h} \tag{21}$$

$$R_{DC} = \frac{X_d(0)}{X_h(0)} \tag{22}$$

In (20), w_d and w_h are the desired first crossover frequency of the lower limb and the actual frequency respectively. In this model, to determine the analytic solution of the crossover frequency is difficult and of little physical meaning, as when the knee is taken into consideration in the model, the multi-joint admittance formulation is complex compared to a simple pendulum-like leg motion as described in many kinds of literature. The two peaks in the resonant response should represent the two relatively independent limbs' frequency, though this is out of our paper's scope, instead, we will focus on the first peak. M_d and M_h are respectively the resonant peak of the desired frequency response and the actual unassisted resonant response.

Thus our design goal is to satisfy the predefined parameters R_w,R_M and R_{DC}. It is shown in Fig.2 how the desired control parameters determine the frequency response of the integral admittance. We specify the control parameters as $R_w = 1.05$,$R_M = 1.20$,$R_{CD} = 1.30$. An intuitionistic present of the modification defined by the three parameters is shown in Fig.2, where the curve is shifted upwards and rightwards.

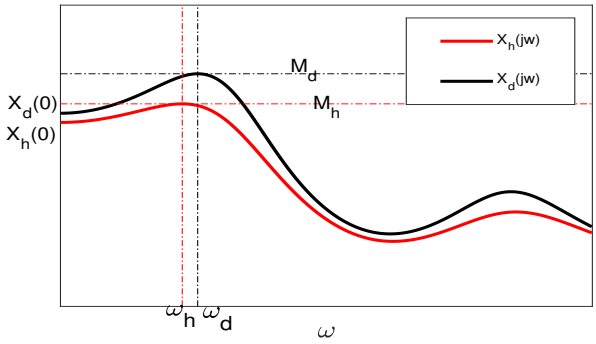

Fig. 2. Frequency response of the unassisted human lower limb's integral admittance $X_h(jw)$ and an desired integral admittance $X_d(jw)$. The chosen control parameters are: $R_w = 1.05$,$R_M = 1.20$,$R_{CD} = 1.30$.

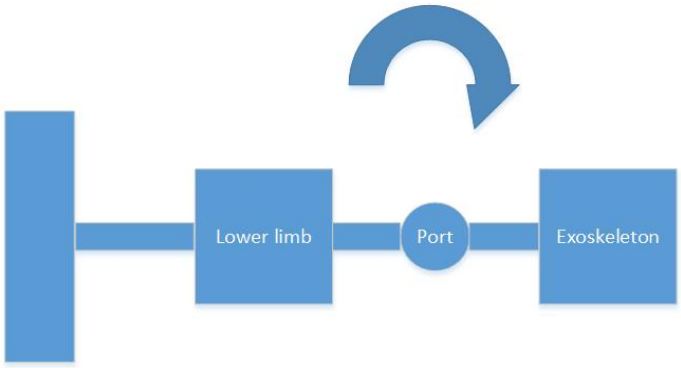

Fig. 3. Model graph of the coupling between lower limbs and the exoskeleton

B. Coupling Model

To meet the assistive goal of the exoskeleton, we should first make the device's mechanism transparent when the device is in the function-off state. In other words, when the user is wearing the exoskeleton, he should feel the as little effect as possible. Moreover, in the walking state, the user should also feel little effect apart from the desired assistive torque. Similar devices have been used in the load helper device BLEEX [4]. Typically, to make the user feel transparent in the inactive stage , an inner-loop control would be introduced to compensate for the inertia, friction, and damping of the mechanism, as well as the gravitational torques [5]. However, addressing this problem is beyond our main goal, in the present formulation we will assume that such inner-loop has already in place.

Notice that we introduce a port mainly to transport the coupled torque. Typically there are two ways to implement with the coupling between the human and the assistive devices, the soft coupling, and the rigid coupling. In our analysis, we assume the coupling is rigid and the coupling torque τ_c is the output torque τ_e. Although they are not exactly the same because of the friction of the machine, belt, and other linking materials, the difference is small enough to be ignored.Under this model, we then assume that the exoskeleton and the thigh have the same angle velocity, $\Omega_e = \Omega_h$. On the basis of this coupling model, the equations of the coupled human-

exoskeleton system are as follows:

$$\Omega_h = Y_h(\tau_h + \tau_e) \tag{23}$$

$$\tau_e = Z_f \Omega_e \tag{24}$$

where Z_f represents the exoskeleton's assistive action. It represents the response of the exerted torque for the exoskeleton's angular velocity. Recall that $\Omega_e = \Omega_h$, we then define the coupled admittance of the lower limb Y_{couple}

$$Y_{couple} = \frac{\Omega_h}{\tau_h} = \frac{Y_h}{1 - Z_f Y_h} \tag{25}$$

C. Loop Shaping Method

In traditional SISO systems that the basic feedback relation can be written as a matrix form:

$$\begin{pmatrix} x_1 \\ x_2 \\ x_3 \end{pmatrix} = \frac{1}{1+PCF} \begin{bmatrix} 1 & -PF & -F \\ C & 1 & -CF \\ PC & P & 1 \end{bmatrix} \begin{pmatrix} r \\ d \\ n \end{pmatrix} \tag{26}$$

where P represents the plant transfer function and C the controller, detailed meaning can be found in [3]. For simplicity, the sensor component F is set to the unit. The stability exerts some limitations for the denominator $1+PCF$, and this will be addressed in later sections. Currently, we focus on the output x_3 as this is of better importance for our target. The matrix above suggests that:

$$x_3 = \frac{PC}{1+PC} r + \frac{P}{1+PC} d + \frac{1}{1+PC} n \tag{27}$$

We know from basic feedback knowledge that x_3 is the actual measure of the output(e.g. the coupled torque in this case). The sensor noise n is circumscribed to the precision and quality of the sensor devices and we will not consider it in the following analysis. Now we pay attention to the rest two components of the measured output, r, and d. As interpreted above, r represents the command input and d the external disturbance. Then the coefficients of these two parameters reflect how the measured output behaves differently when the command input and the external disturbance changes.

Recall that we already have the coupled admittance Y_{couple} as defined in (25), For consistency, we rewrite the coupled admittance as:

$$Y_{couple} = \frac{\Omega_h}{\tau_h} = \frac{Y_h}{1 + Z_f Y_h} \tag{28}$$

Remember that this modification does no harm to the model building, instead provide convenience for our further analysis. From (25) we know the control impedance transfer the exerted torque to the angular velocity, and the overall efforts of this controller contribute to the admittance shaping of Y_h. Recall (27), the external disturbance contributes partly with the coefficient $\frac{P}{1+PC}$, we can easily find the relations between the basic feedback loop and our mechanical admittance.

We define the loop transfer function L as:$L = PC$, we stress that this is an important medium transfer function as our later analysis is based on this function. Along with loop transfer function, we also define the sensitivity transfer function S as: $S = \frac{1}{1+L}$. We then can interpret the coupled mechanical admittance as

$$Y_{couple} = S_h Y_h \tag{29}$$

Where S_h is the sensitivity transfer function:

$$S_h = \frac{1}{1 + Z_f Y_h} \tag{30}$$

Return back to (27), the main component can be extracted out and we can write equivalently $y = \frac{PC}{1+PC} r$, thus the tracking error is

$$e = \frac{r}{1 + PC} \tag{31}$$

So we can interpret the sensitivity transfer function as an index of tracking performance.

Theorem 1: Assume that the feedback system is internally stable and n=d=0. if r is a step, then $e(t) \to 0$ as $t \to \infty$ iff S has at least one zero at its origin.

The proof is a simple application of the final value theorem. Before we step further into the tracking performance, we firstly introduce the ∞-norm of the system.

Remark 1: The ∞-norm of a system is the least upper bound of its absolute value:

$$||u(s)||_\infty = sup_\omega |u(j\omega)|$$

Remark 2: The tracking performance specification is $||W_1 S||_\infty < 1$, Where W_1 is a weighing function. The logic behind it is intuitive as can be seen from the (31). Typically the weighting function is predefined for the specific plant function.

Remark 3: For a known plant, the problem of plant uncertainty should be addressed, where a specific type of unstructured uncertainty is disk uncertainty. We stress this is important for the later robust stability analysis. In this paper, we focus on the multiplicative perturbed form, and other forms are also introduced in [3]. We model the plant uncertainty problem as:

$$\tilde{P} = (1 + \Delta W_2) P \tag{32}$$

The Δ symbol in the equation represents a variable stable transfer function satisfying $||\Delta||_\infty < 1$. W_2 is a fixed weighing transfer function and can be derived hence $||\Delta||_\infty < 1$.

$$|\frac{\tilde{P}(j\omega)}{P(j\omega)} - 1| \leq |W_2(j\omega)| \tag{33}$$

Thus the weighing function W_2 is an upper envelope curve and could be derided through bode graphs by several practices. We should emphasize here this disturbed form of the plant is not the only form, for our multi-joint mechanical admittance, The numerator and the denominator are both polynomials with parameters of damping coefficients and other uncertainty sources, so both can be modeled as a multiplicative perturbed case. Then recall from sensitivity transfer function, we define the corresponding complementary sensitivity function T. This function transfers the command input to the output as suggested from (27).

$$T = 1 - S = \frac{L}{1 + L} \tag{34}$$

At present, We say a controller C provides robust stability if it provides internal stability for every plant considering the

plant uncertainty factors. In our analysis, the plant uncertainty mainly comes from parameters uncertainties such as damping coefficients of the limbs, the inertia and the measurement error of the body.

Theorem 2: A controller C provides robust stability iff $||W_2T||_\infty < 1$

Now we introduce the notion of robust performance. The robust performance refers to the uniformity of the plant performance and stability, which means the internal stability and tracking performance should still hold when the plant function is perturbed. Again in this section, we still use the multiplicative form of perturbation.

Theorem 3: A necessary and sufficient condition for robust performance is $|||W_1S| + |W_2T|||_\infty < 1$

D. Implementation of Control Design

1) Integral feedback for target DC gain: We design the feedback compensator for DC gain mainly to meet the static case of the coupled system. When the coupled exoskeleton with the lower limb is still, this kind of compensator can be regarded as a virtual spring, and the total effect of this compensator is to compensate for the stiffness and gravitational torque [2]:

$$\tau_e = k_{DC}\theta_e \tag{35}$$

Recall from (24) we then obtain the integral feedback controller contributing to part of the impedance controller Z_f:

$$Z_{fDC} = \frac{k_{DC}}{s} \tag{36}$$

To achieve the target DC gain, we make use of the definition of the DC gain ratio and the resonance frequency at static state in both unassisted and assisted case. We can directly derive the value of k_{DC} :

$$k_{DC} = \frac{R_{DC} - 1}{X_h(0)} \tag{37}$$

The term $X_h(0)$ is the frequency response of the lower limb in the static state. Therefore, we can rewrite the controller impedance as a multiplicative form of independent feedback controllers.

$$Z_f = \frac{k_{DC}}{s} Z_f^* \tag{38}$$

Where Z_f^* should satisfy the requirement that

$$Z_f^*(0) = 1 \tag{39}$$

to ensure the DC gain specification is always met. We say this is one aspect of this paper's contribution compared to many other kinds of literature, where DC gain cannot be met in the whole design process [2]. Generally speaking, if we only add a controller like this integral feedback controller, the curve of the frequency response would shift upward. However, Fig.4 shows us even the frequency response shift upwards, the crossover frequency may not increase. Therefore, more should be done to shape the controller impedance Z_f.

Now we reconsider the problem of tracking performance. Initially, our goal is to design the device to assist the human lower limb, but not for tracking. But after the desired DC

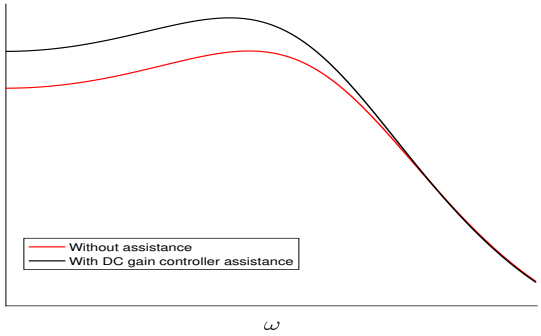

Fig. 4. The frequency response of the coupled system after a DC gain controller is added. The curve has moved upwards, but the crossover frequency decreases instead. An example: R_{DC}=1.1

gain, resonant peak and crossover frequency are introduced, the assistive device can be treated as partly the tracking device, although not rigidly the same. Actually, if we consider the physical phenomenon of the gait, we can easily notice the integral mechanical admittance(i.e. the angle in the time domain) should be the plant output rather than the angular velocity. In that sense, the coupling function will have to change due to the difference in modeling.

2) Lead Compensator: A standard method to increase the crossover frequency is to use a lead compensator. A typical compensator has the form:

$$C(s) = k\frac{s+a}{s+b}, \quad a < b \tag{40}$$

remember in our model, the controller impedance Z_f consists of a DC gain compensator as described above. So we combine this lead compensator into the controller impedance and we get a coupled impedance:

$$Z_f = k\frac{k_{DC}}{s}\frac{s+a}{s+b} \tag{41}$$

Because we need to meet the specific DC gain requirement, we set the constant k as $k = b/a$, this method is temporary here because the internal stability should also be considered. We will maintain the assumption that the system is internally stable for convenience for now. The closer proof will present in the stability analysis later.

3) Stability, Robustness and Performance Assessment: Now our goal is to find the parameters a and b to meet the resonant peak and crossover frequency requirements. Notice that a perfect solution does not always exist due to the inherent limitation of the admittance function. An example is shown in Fig.6 that whether the desired position of the peak point can be reached is partly determined by its distance to the original peak point. But for an assistive device, this distance will not be too far.

In the meantime, to ensure internal stability, it is necessary to make sure that the denominator of the coupled admittance function has no poles in the right-hand side of the complex plane(RHP). Details about stability analysis are given in Section V. We will take the robust stability and the robust performance into consideration first. As put forward

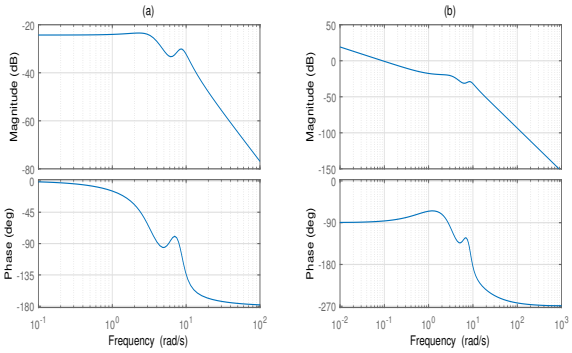

Fig. 5. Control design using a lead compensator with DC gain compensator: (a) Bode plot of Y_h and (b) Bode plot for $L = Y_h Z_f$. An example:$a = 1; b = 10; R_{DC} = 1.1$

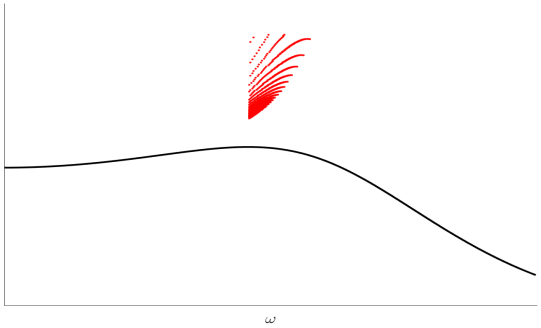

Fig. 6. Range the coefficient in a large scale, and the point representing the crossover frequency and the peak resonant consists of an area with a banana-like lower curve boundary. The range of the coefficients is determined by means of trial and error. Considering our goal of assisting the disabled, the target peak position is bound to a rectangular area. The figure demonstrates the inherent limitation of the mechanical admittance.

in Theorem 3, we can assess the robust stability and robust performance simultaneously, as well as achieve the tracking performance as described in Remark 2.

Remember in (33) we portray the transfer function W_2 as an upper envelope curve in a single multiplicative perturbation situation. But for our mechanical admittance Y_{couple}, the nominator and the denominator are all polynomials with uncertainties resulting from human parameters and damping coefficients. So we should first deduct the equivalent weighing function for robust stability assessment.

Assume W_a and W_b are, respectively the weighing function of the nominator and denominator polynomials of the coupled admittance. The derivation of these two weighting functions is an application of (33).

Theorem 4: Suppose that a nominal plant P is perturbed to

$$\tilde{P} = P\frac{1 + \Delta_a W_a}{1 + \Delta_b W_b} \tag{42}$$

Then the robust stability condition is

$$\| |W_b S| + |W_a T| \|_\infty < 1 \tag{43}$$

Where S and T are transfer function as defined in early parts of this paper. The proof can be found in [3]. We now turn to formulate our design principles:

1) Internal stability, which means there is no RHPs in the denominators of the couple admittance.

2) Target achievement performance, the actual crossover frequency, and the resonant peak should be as close to the desired position as possible.

3) Robustness stability, our index for this criteria is proposed in (43).

To fulfill these three goals simultaneously, and recall that the target position of the peak is not always available, we then introduce a target performance cost function(TPCF), the TPCF goes like this:

$$F = ||w_d - w_{ach}||_\alpha + ||M_d - M_{ach}||_\beta \tag{44}$$

$$[w_{ach}, M_{ach}] = solution(a, b) \tag{45}$$

$$[a, b] \in \mathbb{A} \tag{46}$$

Where $\mathbb{A}$ is pair group whose elements satisfy the internal stability and robust stability as well. The $solution$ represents the computing procedure of our control design, and the w_{ach} and M_{ach} are the achievable peak point position under the parameter pair a and b.

IV. Assistive Control for Lower Limbs: Design Example

A. Loop Shaping Design

In this section, we apply our method to an actual human lower limb. The parameters are chosen according to [1], Where an average of mass and length of limb scale have linear relations with the total human height and weight. The damping coefficients of the human lower limb are the measurement of [6]. We assume the shank shares the same damping coefficient with the thigh. This assumption can be relaxed as we will show in the robustness stability analysis section. We graph the coefficients as Tab. I shows:

TABLE I
Parameters Set Example

Parameter	Meaning	Value
$m_1(kg)$	mass of the thigh	7.165
$m_2(kg)$	mass of the shank	2.800
$l_1(m)$	length of the thigh	0.449
$l_2(m)$	length of the shank	0.429
$a_1(m)$	thigh centroid distance	0.23323
$a_2(m)$	shank centroid distance	0,18221
$b_1(Nm \cdot s/rad)$	hip joint damping coefficient	3.5
$b_2(Nm \cdot s/rad)$	knee joint damping coefficient	3.5

Recall from (19) and $X_h = Y_h/s$, we then remark the mechanical admittance as:

$$Y_h = s\frac{Num}{Den} \tag{47}$$

where Num and Den are both polynomials and represent the numerator and the denominator of the Y_h respectively. We notice the nominator of the integral admittance has a zero at the origin and we will extract the s factor out for simplicity.

TABLE II
TARGET FREQUENCY RESPONSE SPECIFYING

Design parameter	Meaning	Value
R_{DC}	DC gain ratio	1.1
R_{ω}	crossover frequency ratio	1.2
R_M	resonant ratio	1.1

The coupled admittance of the lower limb then can be written in the polynomial form:

$$Y_{couple} = \frac{Num(s+b)}{Dem(s+b) - k_{DC}kNum(s+a)} \tag{48}$$

The internal stability requires that there is no RHPs of the coupled admittance, or equivalently, the denominator of the coupled admittance has no zeros in the right half complex plane. We can calculate the zeros of its denominator numerically. For the controller design, we then follow the steps as described in early sections. We set our target frequency response as in the Tab.II.

As we already have a target DC gain ratio and the lower limb parameter set, we can easily derive the first control parameter k_{DC} from (37). And remember the DC gain ratio can be held in the whole design procedure. Now the key to the control design is to find the control parameter a and b, whose meaning has been illustrated in early sections. We should first decide the norm of the component of the target performance cost function. Notice that the choice of the norm should be consistent with the weighting ratio of the target crossover and target resonant respectively. For design analysis, we normalize the cost function in consideration of the difference in units. We also choose the norm form as $||\cdot||_2^2$. In our design example, the target performance cost function is determined as:

$$F = |\frac{w_{ach} - w_d}{w_d}|^2 + |\frac{M_{ach} - M_d}{M_d}|^2 \tag{49}$$

As suggested above, the target position available under the coupled system is not arbitrary, so for a specific target design, the control parameter may not exactly make the controlled peak position satisfy the target position. Thus the performance target cost function will make a difference. Notice that if a pair of control parameter a and b can just make it happen that the controlled peak position is the target position, then the cost function is zero, so obviously leading to the minimum cost position. Therefore, we have included all cases in the process of control designing. One thing we should keep in mind is that for every possible control pair, the stability of the coupled admittance should be considered at the very beginning. The design results resulting from the design rules are: $a = 1.8$,$b = 18.8$.

B. More Analysis on Stability and Performance

The stability of the coupled system is relatively straightforward as many numerical methods, as well as graphs methods, could show us that the coupled system is stable. Actually, in the process of specifying the control parameters, we have already eliminated the possibility of instability. But for completeness, we will show the stability feature as well

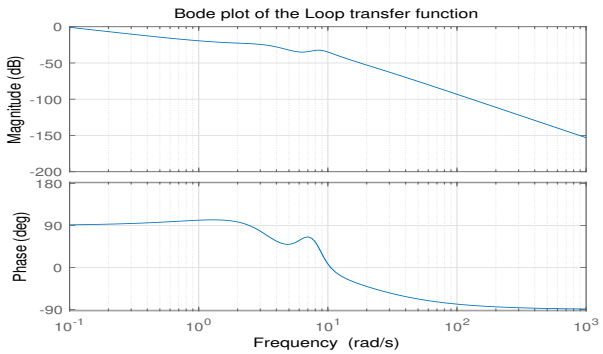

Fig. 7. Bode plot of the loop transfer function, we can know from the curve that this controller has satisfied the requirement of the low-frequency tracking performance and high-frequency robustness stability.

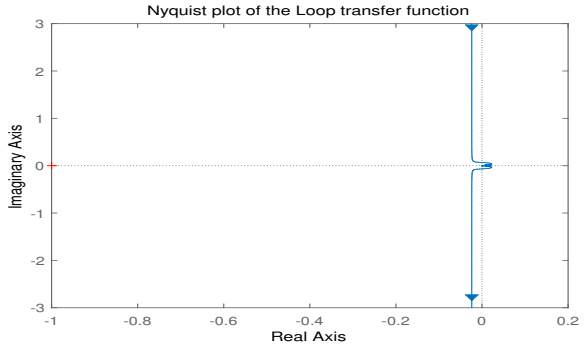

Fig. 8. Nyquist diagram of the loop transfer function $L = Z_f Y_h$

in this section. Remember that our control impedance Z_f has the form

$$Z_f = -\frac{k_{DC}}{s}\frac{b}{a}\frac{s+a}{s+b} \tag{50}$$

We will make use of the Nyquist diagram to show the stability of the coupled system, which mainly measures the distance between the curve and the point $(-1, 0)$ in the complex plane. Recall that the loop transfer function L in this example can be expressed as $L = Z_f Y_h$, and Fig. 7 shows us the loop function provide a good measurement of tracking performance and robustness stability.

C. Performance of the Controller: Frequency Response of the Coupled System

We recall that our main goal of the controller design is to shift the frequency response curve upwards and rightwards. In this subsection, we will present a graph comparing the initial unassisted lower limb frequency and that of the coupled assisted system. From the Fig.9 we know the DC gain has been raised to the exact position, and the crossover frequency and the resonant peak have also been raised to the desired position.

V. ROBUSTNESS STABILITY ANALYSIS

In this section, we will discuss the robustness stability of the coupled lower limb with an exoskeleton. The parameters

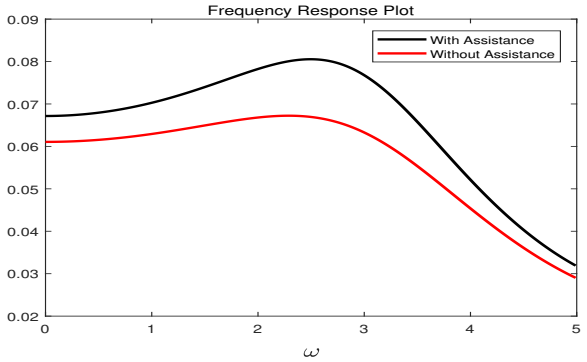

Fig. 9. Comparison between the initial frequency response and the one after coupled with an assistive exoskeleton.

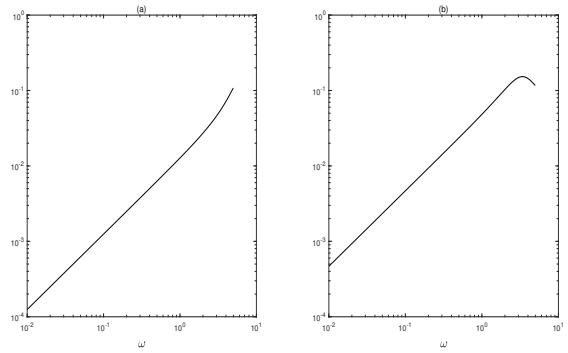

Fig. 10. Bode plot of the weighing transfer function, the range of damping coefficient uncertainty is 3.0-4.0. (a) The weighing function of the nominator; (b) The weighing function of the denominator.

present here inevitably will emerge some kind of uncertainties, such as mass, damping coefficients, length and center positions. For simpleness, we will not go through all cases in this paper, but present an example of robustness stability resulting from the damping coefficients. We choose the damping coefficients because it mainly represents the hindrance effects in the hip joint and the knee joint, together with the effects of the air resistance, which are rather difficult to measure, and the walking gait will bring some difference for the damping coefficients. Remember in early sections we have introduced a way to simultaneously test the robustness stability and the tracking performance, which could be considered separately in low-frequency and high-frequency cases. The test principle is forwarded in (43).

We begin by inferring the possible weighing envelope function of the nominator and the denominator of the coupled mechanical admittance Y_h. Recall that we can use methods of the trail and try to determine the possible weighing function W_a and W_b, which are respectively the envelope weighing function of the nominator and the denominator. Actually, for simplicity, we can just define the weighting function as the infinity norm of the transfer function, in that case, the weighting function is a scaler and cannot illustrate the weighing characteristic facing different frequencies. In this section, we will present a more accurate expression of the weighing function, and the reduction process follows the steps as described in (33),where uncertainties resulting in $\tilde{P}$ is mainly from uncertainties in damping coefficients in our paper's analysis.

We assume the uncertainty of damping coefficients is constrained in a certain range, for example, from 3.0 to 4.0. Notice that this is not a rigid range and we can change it if actual uncertainty ranges exceed the current one. For now, we will temporally assume it right. After some practices of Bode plot, we would easily find that when the damping coefficients introduce some change, the bode plot shift upwards or downwards, thus we could choose the bode plot where the uncertainty is at its boundary of the range as the desired weighing function.

After we have already obtained the weighing function W_a and W_b, we can then test the robustness stability under the criteria of (43), where the sensitivity function and the complementary sensitivity transfer function can be referred in (30) and (34). The robustness test results under the current

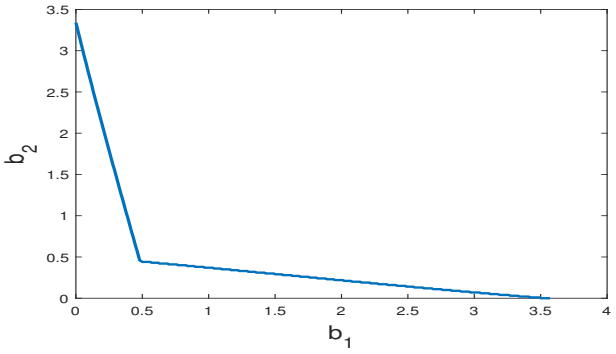

Fig. 11. Boundary curve of the stability, the region above the curve indicates a stable coupled system. The current coefficient pair is (3.5,3.5), which is in the stable area, a small perturbation of the damping coefficient will not cause the system into instability.

coefficient set then can be calculated.

For variety, we can also give a graphical result of the robustness of the system. For stability requirement, the coupled system should have no RHPs, and this is our criteria in this part. Fig.11 shows that the current position of the damping coefficient pair is in a robust position, some small disturb won't cause the coupled system to fall into the instability situation. Therefore, we can safely draw the conclusion that the current position is a stable and robust one.

VI. Simulation

In this part, we apply our control rule into a dynamical walking model. We will show in this part under the assistance of the exoskeleton, the human limb will share a higher natural frequency as well as the amplitude. We assume the human thigh has a sinusoidal swing pattern when walking without external assistance, and the exerted torque between the limb and the exoskeleton can be derived as follows:

$$T = -\frac{k_{DC}b}{a}\int_0^t (\int_0^\tau \theta(\psi)d\psi)(\delta(t-\tau) - (b-a)e^{-b(t-\tau)})d\tau \quad (51)$$

This can be easily proofed using knowledge of Laplace transform, we will not go through this for simplicity. In the simulation, we set the parameters as in the design example

section, where $a = 1.8, b = 18.8, k_{DC} = 1.1$. We compare plots of the torque-time of the assisted case and the transparent case, and the result is clear our loop shaping control methods can raise the natural frequency of the lower limb and the amplitude.

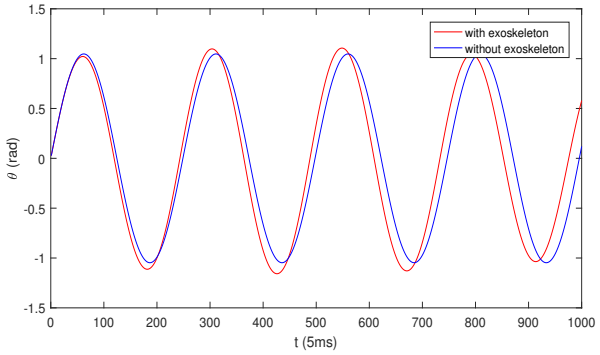

Fig. 12. Plots of the lower limb swing motion, the red line represents the swing motion under exoskeleton assistance while the blue line represents the unassisted case. The time step is 5ms and the angle unit is set as radians.

We can also draw the exerted torque plot of the exoskeleton under our control rule. In our sinusoidal swing motion model, the torque-time relation can be expressed with analytic results, but in the actual human-exoskeleton environment, the torque is computed with numerical methods.

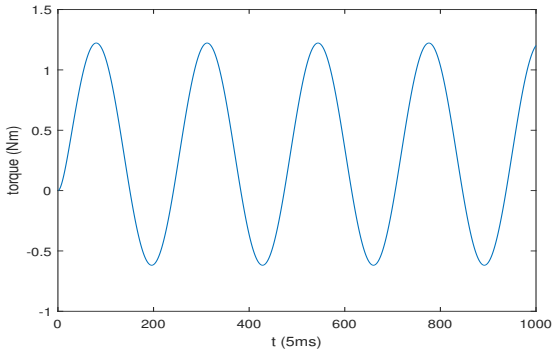

Fig. 13. Exerted torque between the human limb and the exoskeleton.

VII. Conclusion

In this paper, we deduce the double-pendulum model of the lower limb and thus provide the admittance transfer function between the input torque and output angle. In order to make the patient have a better walking performance, the frequency response curve should shift upwards and rightwards. To achieve so, we design an integral feedback controller as well as a lead controller. In the control design procedure, we set three control goals: frequency ratio, resonant ratio, and DC gain ratio. Our control rule can exactly meet the DC gain ratio, and the rest two are met by the numerical optimal solution.

The simulation results show the prospect of this control design approach. In future work, we would apply our method in a real lower exoskeleton and see how it works in rehabilitation. We expect this design approach will provide insight into lower limb exoskeleton control.

References

[1] Artificial limbs. review of current developments. *Physical Therapy*, 36(11):777–778, 1956.

[2] Gabriel Aguirre-Ollinger, Umashankar Nagarajan, and Ambarish Goswami. An admittance shaping controller for exoskeleton assistance of the lower extremities. *Autonomous Robots*, 40(4):701–728, 2016.

[3] John C Doyle, Bruce A Francis, and Allen R Tannenbaum. *Feedback control theory*. Courier Corporation, 2013.

[4] Hami Kazerooni, J-L Racine, Lihua Huang, and Ryan Steger. On the control of the berkeley lower extremity exoskeleton (bleex). In *Robotics and automation, 2005. ICRA 2005. Proceedings of the 2005 IEEE international conference on*, pages 4353–4360. IEEE, 2005.

[5] Tobias Nef, Matjaz Mihelj, and Robert Riener. Armin: a robot for patient-cooperative arm therapy. *Medical & biological engineering & computing*, 45(9):887–900, 2007.

[6] Faryaneh Tafazzoli and M Lamontagne. Mechanical behaviour of hamstring muscles in low-back pain patients and control subjects. *Clinical Biomechanics*, 11(1):16–24, 1996.